Ultrasonics Sonochemistry 20 (2013) 277–286

Contents lists available at SciVerse ScienceDirect

Ultrasonics Sonochemistry

journal homepage: www.elsevier.com/locate/ultson

Ultrasound assisted synthesis of doped TiO_2 nano-particles: Characterization and comparison of effectiveness for photocatalytic oxidation of dyestuff effluent

S.R. Shirsath [a], D.V. Pinjari [c], P.R. Gogate [c], S.H. Sonawane [b,*], A.B. Pandit [c]

[a] Department of Chemical Engineering, Vishwakarma Institute of Technology, 666 Upper Indira Nagar, Pune 411037, India
[b] Chemical Engineering Department, National Institute of Technology, Warangal, AP 506007, India
[c] Chemical Engineering Division, Institute of Chemical Technology, Matunga, Mumbai 400019, India

ARTICLE INFO

Article history:
Received 22 February 2012
Received in revised form 14 May 2012
Accepted 25 May 2012
Available online 13 June 2012

Keywords:
Titanium dioxide
Photocatalyst
Doping
Characterization
Ultrasound
Dye degradation

ABSTRACT

The present work deals with the synthesis of titanium dioxide nanoparticles doped with Fe and Ce using sonochemical approach and its comparison with the conventional doping method. The prepared samples have been characterized using X-ray diffraction (XRD), FTIR, transmission electron microscopy (TEM) and UV–visible spectra (UV–vis). The effectiveness of the synthesized catalyst for the photocatalytic degradation of crystal violet dye has also been investigated considering crystal violet degradation as the model reaction. It has been observed that the catalysts prepared by sonochemical method exhibit higher photocatalytic activity as compared to the catalysts prepared by the conventional methods. Also the Ce-doped TiO_2 exhibits maximum photocatalytic activity followed by Fe-doped TiO_2 and the least activity was observed for only TiO_2. The presence of Fe and Ce in the TiO_2 structure results in a significant absorption shift towards the visible region. Detailed investigations on the degradation indicated that an optimal dosage with 0.8 mol% doping of Ce and 1.2 mol% doping of Fe in TiO_2 results in higher extents of degradation. Kinetic studies also established that the photocatalytic degradation followed the pseudo first-order reaction kinetics. Overall it has been established that ultrasound assisted synthesis of doped photocatalyst significantly enhances the photocatalytic activity.

1. Introduction

Over the last decade different catalytic techniques have been investigated as a possible solution for the ever increasing serious environmental pollution problems. Heterogeneous photocatalysis is a well accepted technique with a great potential to control aqueous contaminants or air pollutants. Among various oxide semiconductor photocatalysts, titanium dioxide has attracted interest of many researchers in recent years because of its applicability for all the three classes of water contaminants viz., organic, inorganic and microbiological with a minimal risk of the production of harmful byproducts [1–5]. Titanium dioxide has been proven to be the most suitable photocatalyst because of its chemical inertness, strong oxidizing power, long-term stability against photo and chemical corrosion, suitable band gap energy and electronic and optical properties. Also titanium dioxide is photocatalytically stable, relatively easy to produce and is able to efficiently catalyze reactions [6–9]. It is also used in cosmetics, paints, electronic paper, filter materials, anti-reflection films, sensors, and dye-sensitive solar cells [10,11].

Undesirable recombination of electrons and holes, and low efficiency under irradiation in the visible region are the two main drawbacks associated with the use of TiO_2 for environmental applications [12,13]. Efforts have been made to extend the light absorption range of TiO_2 from UV to visible light and to improve the photocatalytic activity of TiO_2 [14]. The current research on nanoscience and nanotechnology has been oriented towards the fabrication, characterization, and manipulation of novel materials, broadly referred as nanocomposites, which can be used as catalysts, adsorbents and sensors in optical, electronic and magnetic devices [15]. Dopants, such as transitional metals can be added to TiO_2 to improve its catalytic activity and also reduce the recombination of photo-generated electrons and photo-generated holes. Noble metals doped or deposited on TiO_2 also show effect on the photocatalytic activity by extending excitation wavelength from the UV to the visible light range [11–14,16,17].

There have been many reports of transition metals (Fe, Al, Ni, Cr, Co, W, V and Zr), metal oxides (Fe_2O_3, Cr_2O_3, CoO_2, MgO + CaO and SiO_2), transition metal ceramics (WO_3, MoO_3, Nb_2O_5, SnO_2 and ZnO) and anionic compounds (C, N, and S) being used to dope TiO_2 to improve its applicability [2,18–20]. Zeleska [21] has reviewed the preparation methods of doped TiO_2 with metallic and

* Corresponding author. Address: Department of Chemical Engineering, National Institute of Technology, Warangal, AP 506004, India. Tel.: +91 790 2462626.
E-mail addresses: pr.gogate@ictmumbai.ac.in (P.R. Gogate), shirishsonawane@rediffmail.com (S.H. Sonawane).

1350-4177/$ - see front matter © 2012 Elsevier B.V. All rights reserved.
http://dx.doi.org/10.1016/j.ultsonch.2012.05.015

nonmetallic species, including various types of dopants and doping methods. Rauf [14] has given an overview on the photocatalytic degradation of azo dyes in the presence of TiO_2 doped with selective transition metals.

Higher catalytic activity has been reported for the Ce and CeO_2 doped TiO_2 materials for photo-degradation of dyes and other pollutants [13,22,23]. Titanium dioxide nanopowders doped with visible responsive catalyst may shift the UV absorption threshold of TiO_2 into visible spectrum range and photocatalytic activities can be higher than those of pure TiO_2 and Degussa P25 [6,24–27]. Effect of silver, platinum and gold doping on the TiO_2 for photocatalytic reduction of CO_2 and sonophotocatalytic degradation of methyl orange and organic pollutant nonylphenol ethoxylate has been investigated [7,15,16,28]. Also there are reports of tin, calcium, sulfur and zirconia doped TiO_2 being used for photo-degradation of model pollutants [29–32].

The synthesis of metal-loaded semiconductor oxide materials by conventional physical blending or chemical precipitation followed by surface adsorption usually yields insoluble materials for which the control over size, morphology and dispersion of the metal component remains inherently difficult. These methods often require a long time and are inherently multi-step procedures. Sonochemistry has been proven to be an excellent method for the preparation of mesoporous materials. The physical and chemical effects generated by acoustic cavitation can be expected to significantly influence the properties of doped materials [6,15]. Ultrasound has been very useful in the synthesis of a wide range of nanostructured materials, including high-surface area transition metals, alloys, carbides, oxides, and colloids. The collapse of cavitation bubbles generates localized hot spots with transient temperature of about 10000 K, pressures of about 1000 atm or more and cooling rates in excess of 10^9 K/s. Under such extreme conditions, various chemical reactions and physical changes occur and numerous nano-structured materials such as metals, alloys, oxides and biomaterials can be effectively synthesized with required particle size distribution [6,33–35]. In the past the sonochemical method has been applied to prepare various TiO_2 and doped nanomaterials and photocatalytic activity has been evaluated by different researchers [36–41].

Yu et al. [37] synthesized pure TiO_2 particles using ultrasonically-induced hydrolysis reaction and compared the photocatalytic activity of prepared samples with Degussa P 25 and samples prepared by conventional hydrolysis method. Neppolian et al. [39] also prepared nano TiO_2 photocatalysts using sol–gel and ultrasonic-assisted sol–gel methods using two different sources of ultrasonicator, i.e., a bath type and horn type. The effect of ultrasonic irradiation time, power density, the ultrasonic sources (bath-type and horn-type), magnetic stirring, initial temperatures and sizes of the reactors has been investigated. Li et al. [38] used the combination of ultrasonic and hydrothermal method for preparing Fe-doped TiO_2 for photo-degradation of methyl orange. Zhou et al. [6] used ultrasonicaly-induced hydrolysis reaction for the preparation of Fe-doped TiO_2 whereas Huang et al. [36] synthesized and characterized Fe_xO_y–TiO_2 via the sonochemical method.

As mentioned earlier there are many reports of Fe doping on TiO_2 to improve its photocatalytic activity. Amongst a variety of transitional metals, iron has been considered to be an appropriate material due to the fact that the radius of Fe^{3+} (0.79 Å) is similar to that of Ti^{4+} (0.75 Å), so that Fe^{3+} can be easily incorporated into the crystal lattice of TiO_2. Fe^{3+} has proved to be a successful doping element due to its half-filled electronic configuration [2,6,24,26,27]. Cerium oxides have attracted much attention due to the optical and catalytic properties associated with the redox pair of Ce^{3+}/Ce^{4+}. Ce-doped TiO_2 materials have been synthesized by the sol–gel and hydrothermal methods and used in the photocatalytic degradation applications. But there are very few reports on Ce doped catalysts and the beneficial effect of Ce doped TiO_2 catalysts are known to depend on different factors, such as the synthesis method and the cerium content. [13,22,23]. The photocatalytic performance of TiO_2 catalysts depends strongly on the methods of metal ion doping and the amount of doping material, since they have a decisive influence on the properties of the catalysts. Therefore, it is necessary to investigate the effects of doping method and doping material content on the photocatalytic performance of TiO_2 nanocatalysts.

The present work deals with a detailed study about establishing the influence of ultrasound on the phase composition, structure and performance of pure and doped TiO_2 nanocatalysts. Cerium and Fe-doped TiO_2 nanocatalysts with different amounts of doping elements were prepared by a single-step sonochemical method and conventional method at room temperature. Photocatalytic activity of the prepared composites has been evaluated for the degradation of crystal violet dye. Dye stuffs are a ubiquitous class of synthetic organic pigments that represent increasing environmental issues. As a widely used cationic triphenylmethane dye, crystal violet has high stability because of the electron-donating groups in its unique structure. Crystal violet is a non-biodegradable mutagen and mitotic poison and hence is associated with considerable environmental and health concerns. Considering the Indian context, crystal violet is extensively used in industries such as textile, paper, leather, additives, foodstuffs, cosmetics, and analytical chemistry. Considering the widespread use and toxic nature, it was thought imperative to evaluate the degradation patterns and hence crystal violet has been selected as a model pollutant.

2. Experimental

2.1. Materials

Titanium isopropoxide, propanol, cerium nitrate, and ferric nitrate were procured from S. D. Fine Chemicals Ltd., Mumbai, India. Sodium hydroxide was obtained from Merck Ltd., Mumbai, India. Crystal violet dye was procured from M/s., CDH, India. All the chemicals were of analytical grade and were used as received from the supplier. Freshly prepared distilled water was used in all the experiments.

2.2. Synthesis of TiO_2 by conventional method (CV)

Cerium (III) nitrate, Ferric nitrate and titanium (IV) isopropoxide were used as precursors and 2-propanol was used as solvent. In conventional synthesis procedure, 50 ml of 2-propanol was taken in a 250 ml beaker and 5 ml of titanium isopropoxide was added at room temperature (35 ± 2 °C). The beaker was placed in a constant temperature bath. Solution of cerium nitrate was prepared in 20 ml distilled water. Sodium hydroxide was dissolved in 50 ml distilled water separately and 5 ml of sodium hydroxide solution and 2 ml of cerium nitrate solution were added simultaneously to the titanium isopropoxide solution in propanol after every 30 s until a total of 50 ml sodium hydroxide solution and 20 ml of cerium nitrate solution were added into the beaker. After the addition of all the chemicals, the reaction was allowed to proceed for 4 h under stirring at a temperature of 35 ± 2 °C. After 4 h, the resulting precipitate was centrifuged, filtered, dried and calcined at 450 °C for 3 h. For preparing Fe doped TiO_2, ferric nitrate was used as iron precursor and similar procedure was followed. The catalysts prepared by this method are hereafter named as TiO_2 (CV), Fe–TiO_2 (CV) and Ce–TiO_2 (CV) where CV stands for conventional method of preparation. Pure TiO_2 sample was prepared according to the above procedure without the addition of cerium/iron precursor.

2.3. Synthesis of TiO_2 by sonochemical method (US)

In a typical synthesis procedure involving ultrasound, 50 ml of 2-propanol was taken in a 250 ml beaker and 5 ml of titanium isopropoxide was added. The beaker was placed in a constant temperature bath and the sonication was carried out by employing a direct immersion titanium horn in the sonication cell. Solutions of five different concentrations of cerium nitrate were prepared to get 0.4, 0.8, 1.2, 1.6 and 2 (mol%) of Ce to TiO_2 in 20 ml distilled water. 5 ml of sodium hydroxide solution and 2 ml of cerium nitrate solution were added simultaneously after every 30 s till a total of 50 ml sodium hydroxide solution and 20 ml of cerium nitrate solution were added into the ultrasound reactor. After the addition of all the solutions, the mixture was sonicated for further 30 min. After 30 min of irradiation the solution was kept undisturbed for settling of the precipitate. The resulting precipitate was centrifuged, filtered, dried and calcined at 450 °C for 3 h. Similar procedure was adopted for the synthesis of Fe doped TiO_2 nanocatalyst with molar ratios of 0.4, 0.8, 1.2, 1.6 and 2 (mol%) of Fe to TiO_2. Pure TiO_2 sample was also prepared according to the above procedure except the addition of cerium/iron precursor. Synthesis procedure for cerium doped TiO_2 is schematically shown in Fig. 1. An ultrasonic horn has been used as a source of ultrasonic irradiations for the synthesis of TiO_2 doped composite. The specifications of the horn are as follows: Make: Sonics and Materials, USA; Operating frequency: 22 kHz; rated output power: 750 W; diameter of stainless steel tip: 1.3×10^{-2} m, surface area of ultrasound irradiating face: 1.32×10^{-4} m^2, expected ultrasound intensity: 3.4×10^5 W/m^2 and the horn was operated at 40% amplitude. The catalysts prepared by this method are hereafter described as TiO_2 (US), Fe–TiO_2 (US) and Ce–TiO_2 (US) where US stands for sonochemical method of preparation. The experimental set up for the sonochemical synthesis is schematically shown in Fig. 2.

The reaction time required for the conventional synthesis was 4 h while during sonochemical synthesis the precipitate was formed within 30 min. Zhou et al. [6] has investigated the ultrasound assisted synthesis of Fe doped TiO_2 and reported that the reaction time was observed to be 45 min at 20 °C temperature. The reduction in the reaction time compared to conventional synthesis is due to the cavitational effect. Further, the rapid micromixing and implosive collapse of bubbles in a liquid solution results in extremely high temperatures during ultrasound induced hydrolysis, which results into accelerated hydrolysis reaction.

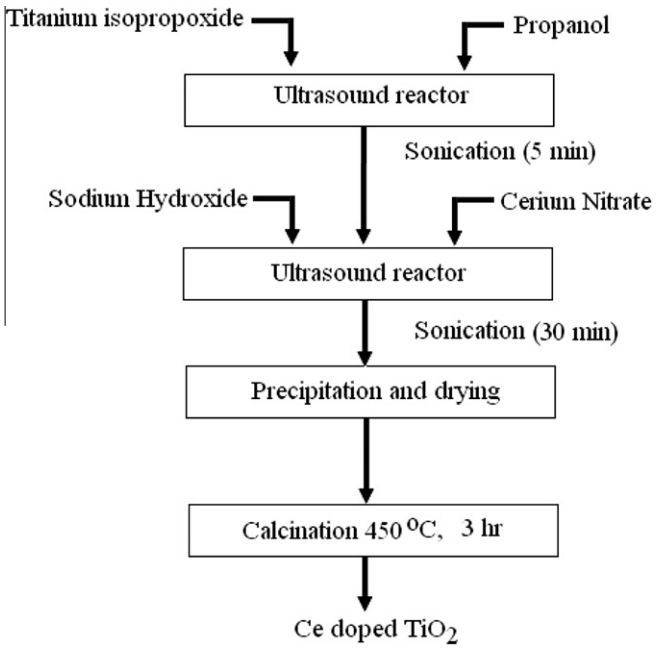

Fig. 1. Synthesis of Ce doped TiO_2 by sonochemical method.

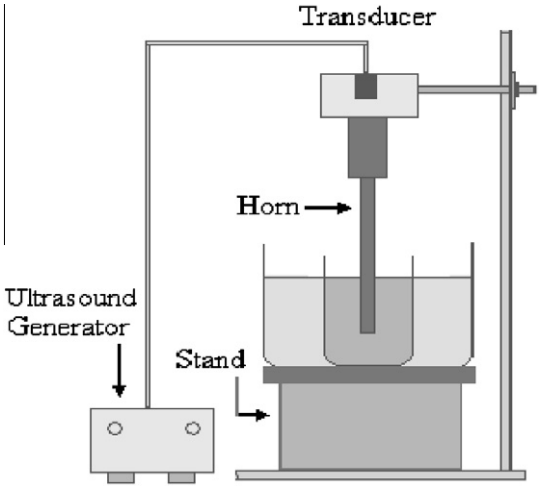

Fig. 2. Experimental setup for sonochemical synthesis.

2.4. Characterization of TiO_2 catalysts

XRD diffraction patterns of TiO_2 samples were recorded by means of powder X-ray diffractometer (Philips PW 1800). The XRD patterns were recorded at angles between 20° and 70° with a scan rate of 2°/min. FTIR Spectra of the samples were recorded on Perkin Elmer FTIR spectrometer (Paragon 1000 PC) in the wave number range of 500–4000 cm^{-1}. Transmission electron microscopy (TEM, magnification 7,50,000×) image was taken on a Philips Tecnai 20 model.

2.5. Photocatalytic degradation experiments

In order to compare the photocatalytic activity of synthesized catalysts, crystal violet dye degradation studies have been carried out in a laboratory scale reactor. The solution was irradiated in a closed box with a UV lamp Spectroline XX-15 N which emits radiation at 365 nm with intensity of 2000 W/cm^2. All the photocatalytic degradation experiments were carried out at a pH of 6.5 which is the natural pH of the crystal violet solution and the temperature was maintained at 35 °C. The effect of various operating parameters such as catalyst loading and initial dye concentration was studied for the different photocatalysts. For all experiments, 150 ml of crystal violet dye solution was taken in a beaker and appropriate quantity of catalyst was added.

Initially, the time required for reaching the adsorption equilibrium as well as the maximum amount of dye adsorbed on the TiO_2 surface under dark and stirred conditions was established using preliminary studies prior to the actual experiments (using UV irradiations). The mixture was stirred with magnetic stirrer for 120 min in the dark to establish the equilibrium adsorption characteristics. The results indicated that maximum of 1.5% of crystal violet dye could be adsorbed on the TiO_2 (0.3 g/l loading) and adsorption equilibrium was obtained within 15 min of contact time. The absorbance value did not change with extended time of contact beyond 15 min. Considering this observation, all the photocatalytic degradation experiments have been carried out with 15 min of soaking period under stirring. The time duration of 15 min matches with the studies related to the degradation of methyl orange reported elsewhere [7]. After the attainment of adsorption equilibrium, the suspensions were irradiated with UV

lamp at constant stirring speed. Samples were withdrawn regularly from the reactor and centrifuged prior to analysis, in order to separate any suspended solids. UV–vis spectrophotometer (SHIMADZU 160A model) was used to determine the concentration of crystal violet dye. The wavelength of maximum absorbance (λ_{max}) of dye was found to be 590 nm. Demineralized water was used as a reference.

Reproducibility of the obtained experimental data is very important in investigation related to the effects of the operating parameters. In the current work, all the experiments were carried out at least two times to estimate the reproducibility of the obtained data. The graphs were plotted using mean values obtained from the data. The standard deviation of the replicate values is shown as error bars in the values depicted on *Y* axis. All the experimental errors were found to be within ±4% of the mean reported value.

3. Results and discussion

3.1. XRD analysis of pure and doped TiO_2 nanoparticles prepared by conventional and sonochemical method

The wide angle X-ray diffraction pattern was used to investigate the phase structures of the prepared TiO_2 powders. Fig. 3 shows the XRD patterns of the TiO_2 powder samples prepared by ultrasonic method and the conventional method. Neat TiO_2 prepared by both the methods, shows the presence of the main peaks at $2\theta = 25.2°$, 38°, 47.6°, 55.1° and 61.9° and hence confirms that the catalysts have been predominantly crystalline in nature with anatase as the major phase. For Fe doped TiO_2 nanoparticles the mole ratio of Fe/Ti was 2% for both the methods. The XRD patterns for Fe doped TiO_2 prepared by both the methods showed the peaks at $2\theta = 25.8°$, 36.9°, 48.1°, 54.1° and 62.4° corresponding to the anatase phase and hence it can be established that doping with metal ions did not influence the crystal structure of the TiO_2 particle. The XRD pattern also showed the peaks at 34.4° which can be assigned to the presence of Fe in hematite form in TiO_2 [10,18]. Similarly the XRD patterns of Ce doped TiO_2 for Ce/Ti molar ratio of 2% showed the presence of main peaks at $2\theta = 25.4°$, 37.4°, 47.8°, 54.5° and 62.7° again corresponding to the anatase phase. Compared with JCPDS card No. 21–1272 data files, it was found that all peaks observed in the XRD patterns are consistent with anatase (101), (004), (200), (211) and (204) spacing, respectively [2,4,11,13,31]. In addition, a broad peak was observed at $2\theta = 29.1°$. Some of literature reports indicate that the Ce-doped TiO_2 materials shows the presence of prominent peaks at 30° and 30.6° which are assigned to cerium titanate–Ce_x $Ti_{(1-x)}$ O_2 [13,42]. Thus, in the present case as there was no peak observed at 30°, peak corresponding to 29.1° can be assigned to the presence of cerium as a separate cubic CeO_2, or as cerium titanate in the TiO_2 phase. From the figure, it is also found that the intensities of peaks prepared by sonochemical method are higher as compared to the conventional method and also the peaks are sharper. This clearly indicates the increase in the crystallinity of TiO_2, Fe and Ce doped TiO_2 nanoparticles prepared with sonochemical method leading to the enhanced formation of crystalline particles with anatase phase.

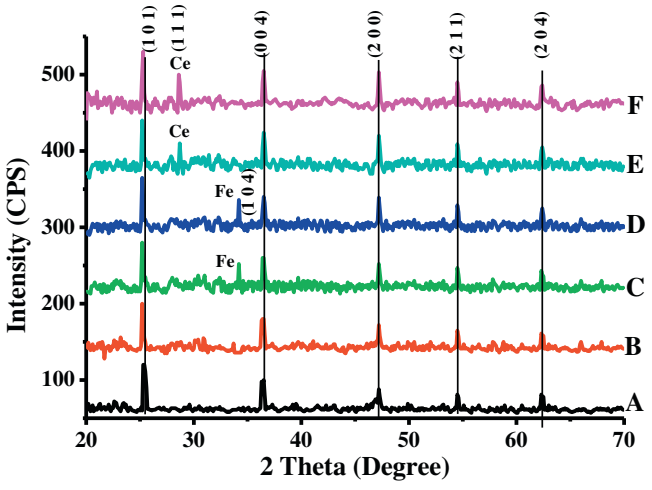

Fig. 3. XRD patterns of Ce-doped TiO_2, Fe-doped TiO_2 and undoped TiO_2 powder prepared by conventional and sonochemical method [A – TiO_2 (CV), B – TiO_2 (US), C – Fe–TiO_2 (CV), D – Fe–TiO_2 (US), E – Ce–TiO_2 (CV), F – Ce–TiO_2 (US)].

3.2. FTIR analysis of pure and doped TiO_2 nanoparticles prepared by conventional and sonochemical method

The FTIR spectra of pure TiO_2 and doped TiO_2 nanoparticles prepared by sonochemical method are shown in Fig. 4. The absorption bands in the region of 3420–3450 cm^{-1} are generally assigned to the stretching vibrations whereas the bands in the region 1630–1640 cm^{-1} are assigned to the bending vibrations of the hydroxyl on the surface of TiO_2 catalysts [9,17,43]. The absorption bands in the region of 520–580 cm^{-1} are assigned to the stretching vibration of Ti–O. In the present work, results of FTIR analysis shows four main absorption peaks located in the regions 482–507, 1687–1760, 2360–2393, 3568–3651 cm^{-1}. The absorption bands in the region of 1687–1760 cm^{-1} are attributed to the bending vibration of the hydroxyl on the surface of TiO_2-based catalysts, while the bands in the region of 3568–3651 cm^{-1} may be assigned to the stretching vibration of the hydroxyl on the surface of the catalysts, since there were no absorption peaks in the region of 3420–3450 cm^{-1}. The absorption bands in the region of 482–507 cm^{-1} can be assigned to the stretching vibration of Ti–O. In addition, peaks in the range of 883–945 cm^{-1} are observed. These peaks can be assigned to the main band (944 cm^{-1}) corresponding to TiO_2 [13]. No additional peaks are present upon Fe and Ce doping, supporting the efficient dispersion of doping elements.

3.3. UV–visible absorption spectra of pure and doped TiO_2 nanoparticles

The increase in the absorption in the visible region depends not only on the type of dopant but also on the method of preparation. The method of preparation plays a significant role in controlling the properties of the TiO_2 nano-particles which could be identified using UV spectroscopic analysis. Fig. 5 shows the UV–visible spectra of the pure TiO_2 and doped TiO_2 samples prepared by using

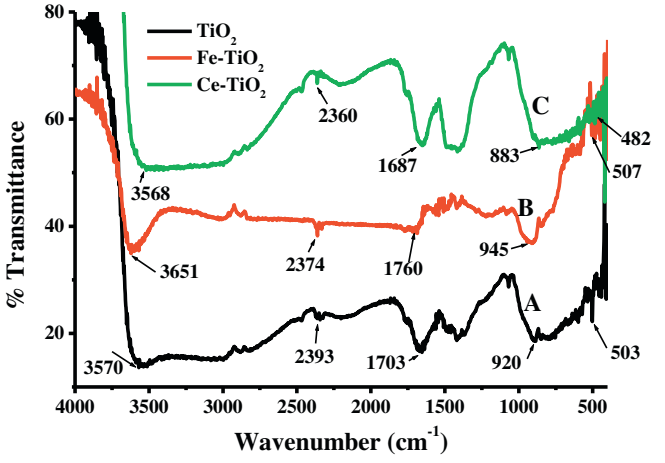

Fig. 4. FTIR spectra of (A) Pure TiO_2, (B) Fe–TiO_2, and (C) Ce–TiO_2 synthesized by sonochemical method.

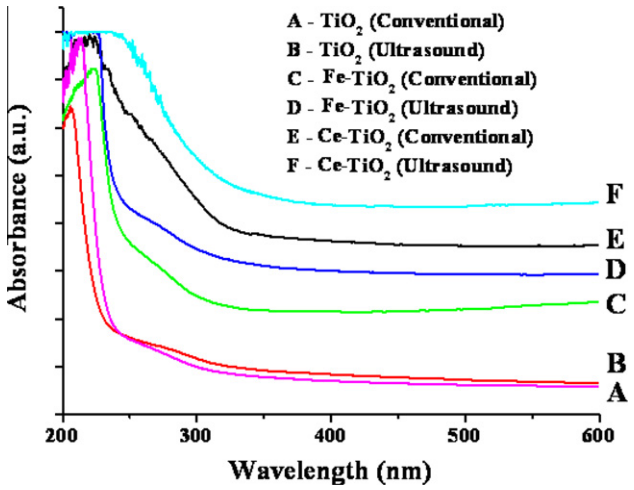

Fig. 5. UV–vis spectra of pure and doped TiO_2 nanoparticles prepared by conventional and sonochemical method.

conventional and sonochemical methods. It is well known that the absorption at wavelength of less than 387 nm is caused by the intrinsic band gap absorption of TiO_2. Usually, metal ion doping affects the light absorption characteristics of TiO_2. The introduction of dopants not only shifts the absorption edge towards the visible region but also increases the absorption of TiO_2 in whole of the visible range (higher wavelength 400–600 nm) [1,2,6,27]. It can be seen from the Fig. 5 that each sample has a broad intense absorption below 400 nm which is the characteristic absorption of TiO_2 corresponding to the excitation of electrons from the valence band to the conduction band in the anatase TiO_2. In the visible region (>400 nm) Ce-doped TiO_2 samples exhibit red shifts of absorption edge and significant enhancement of light absorption at 400–600 nm which is higher than pure TiO_2. The red shift of the absorption spectra could be ascribed to the broad absorption band of transition metals and rare earth elements, and the effect of doping into pure TiO_2 was similar to the influence of adding a photosensitizer to the reaction solution. Further, the enhancement in the absorption could also be due to the adsorption/ deposition of doping elements on TiO_2 particles clearly indicating a decrease in the band gap energy of TiO_2 [44]. This extended absorbance indicates the possible enhancement in the photocatalytic activity of prepared samples. A crystal violet molecule can be degraded into aryl compounds representing the photo oxidation activity. Though, it has been presumed that the doping gives the visible light effect, it is important to note here that the UV light effect is more dominant than the visible light as UV light activated photocatalytic reaction is more pronounced [45].

Fig. 5 also clearly shows the influence of doping and the preparation method on the UV–vis absorption. Modification of TiO_2 with Fe, Ce ions significantly affected the absorption properties of photocatalysts, whereas for pure TiO_2 particles there was no significant increment in the absorption using ultrasound assisted method as compared to the conventional method. However for doped TiO_2 particles, higher absorption was shown by the particles prepared by sonochemical method. For Ce–TiO_2 samples the absorbance in the visible range was increased by 15% as compared to the samples prepared by conventional method.

3.4. TEM analysis and particle size distribution of TiO_2 and doped TiO_2 nanoparticles

Fig. 6 illustrates the transmission electron microscopy (TEM) images of pure TiO_2 (A), Fe doped TiO_2 (B) and Ce doped TiO_2 (C) nanoparticles prepared by sonochemical method. Spherical TiO_2 particles were formed by the sonochemical method. During ultrasonic irradiation, microjets formed due to the cavitational activity helps to form the resultant inorganic oxide particles with smaller and more uniform particles size. The particle were formed with a fairly narrow size distribution and uniform shape could be observed. The primary particle size of sonochemically synthesized TiO_2, Ce–TiO_2 and Fe–TiO_2 nanoparticles was in the rage of 10–50 nm and the individual particles aggregated to form secondary particles of larger size. Further the particle size of pure TiO_2 (Fig. 6A) is large as compared to the doped TiO_2. The crystallite size decreased because of the doping, which implied that Fe, Ce doping restrained the increase in grain size and refined the crystallite size. Moreover the decrease in the particle size is due to an increase in the microstrain effect. The increase in the microstrain may be because of the metal introduction into the anatase lattice and the associated generation of oxygen vacancies [46]. Nahar et al. [24] used impregnation and calcination method for the preparation of Fe doped TiO_2 nanoparticles and reported that the particle size was in the range of 1–2 μm. In the present study, the particle size is found to be around 10–50 nm, which is significantly lower than that obtained in the work of Nahar et al. [24]. The observed trends can be attributed to the fast kinetics of the ultrasound assisted

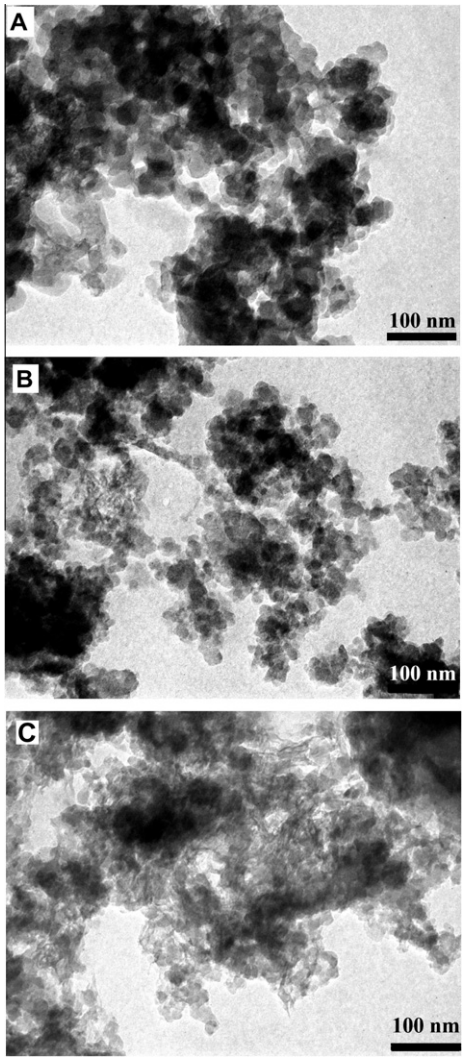

Fig. 6. TEM images of (A) pure TiO_2, (B) Fe doped TiO_2 and (C) Ce doped TiO_2 nanoparticles prepared by sonochemical method.

reaction providing insufficient time for particle nucleation and growth [47].

The particle size distribution of the samples prepared by sonochemical method and conventional method has been depicted in Fig. 7. All the samples prepared by sonochemical method showed smaller particle size whereas for the synthesis using conventional method, the size was found to be larger. The average particle size of undoped TiO_2 prepared by sonochemical method is found to be 197 nm whereas the average particle size of Fe and Ce doped TiO_2 for sonochemical method is observed to be 169 and 157 nm respectively. The average particle size of undoped TiO_2 prepared by conventional method was found to be 298 nm.

3.5. Photocatalytic activity of the catalysts for degradation of dye

The photocatalytic activity of the prepared samples was tested for the degradation of crystal violet dye. The effect of different operating parameters such as effect of preparation method, doping material content, catalyst loading and effect of initial dye concentration on the extent of degradation was investigated and has been discussed in the following sections.

3.5.1. Effect of preparation method and irradiation time

Fig. 8 shows the change in the absorption spectra of crystal violet dye with different irradiation times catalyzed by TiO_2. The aqueous solution of crystal violet dye (30 mg/L) shows a major absorption band at 590 nm. After achieving the equilibrium (soaking time under stirring), the change in the extent of degradation was observed with an increase in the UV irradiation time. With UV irradiation time increasing from 0 to 120 min, the absorption decreased gradually and the peak intensity at 590 nm also decreased. The initial peak intensity (after reaching the adsorption equilibrium) was found to be the maximum at 590 nm as expected. It was also observed that the extent of decrease in the absorption peak was lower at higher treatment times. This may be because of the formation of intermediates and their competitiveness with parent dye molecules in the photocatalytic degradation process. The slow kinetics of dye degradation after certain time limit can also be attributed to the difficulty in converting the N-atoms (N-demethylated products) of dye into oxidized nitrogen compounds [48]. Also, hydroxyl radicals **.**OH can attack different electron rich sites such as N–C bonds, phenyl rings and the central carbon atom of CV in non-effective way with increased treatment times [49]. To find out the maximum possible degradation, initially the experiments were conducted for 180 min and it was found that there was no appreciable degradation after 120 min irradiation. Hence all the experiments were carried at a constant treatment time as 120 min.

To study the effect of preparation method on the photocatalytic activity of the catalysts prepared by sonochemical and the conventional method, the experiments were conducted for 2% (mol%) of Ce and Fe doped TiO_2 and pure TiO_2. Fig. 9 shows the relative concentration (C/C_o) of dye with UV irradiation time (C_o is the concentration after achieving the adsorption equilibrium) for the initial dye concentration of 30 mg/L and the catalyst loading of 0.2 g/L. It is observed that the degradation of crystal violet increased gradually with UV irradiation time for all the samples. The highest degradation (84%) was achieved with Ce–TiO_2 (US) sample followed by Fe–TiO_2 (US) (77%) and undoped TiO_2 (US) sample gave 71% degradation. The samples prepared by conventional method resulted in 75, 68 and 61% degradation for Ce–TiO_2(CV), Fe–TiO_2(CV) and TiO_2(CV) respectively. Maximum extent of degradation for the Cerium doping can be attributed to the fact that cerium shows the enhanced photo-response in the visible region and the redox pair of cerium (Ce^{3+}/Ce^{4+}) is also important, since cerium could act as an effective electron scavenger to trap the bulk electrons in TiO_2 [13]. The preparation method played an important role in deciding the photoactivity of a catalyst. It was observed that the catalysts prepared by sonochemical method showed higher activity against catalyst prepared by the conventional method, possibly attributed to the higher surface area for the reaction due to the lower particle size of the catalyst achieved with the sonochemical method. The increased high-velocity interparticle collisions among the particles can result in the fragmentation of the TiO_2 particles leading to lower size in the case of sonochemical method. Also ultrasonic irradiation may accelerate the hydrolysis and formation of titania crystals. Further sonication method can evenly disperse the metal ions into the crystal lattice of TiO_2, independent of whether the ions react with Ti–gel or not [36]. This study clearly demonstrates the importance and advantages of sonication in the modification and improvement of the photocatalytic properties of TiO_2 and doped TiO_2 catalysts. After the first set of experiments, as it was observed that all the samples prepared by sonochemical method gives higher degradation than the samples prepared by conventional method, the studies related to the effect of other operating parameters on the degradation process were performed with the catalyst prepared by sonochemical method.

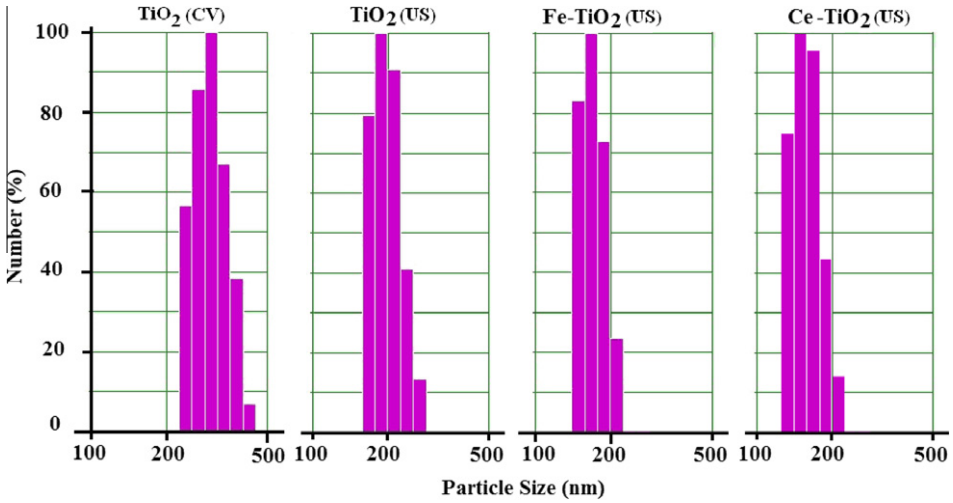

Fig. 7. Particle size distributions of Fe–TiO_2, Ce–TiO_2 and TiO_2 synthesized by sonochemical and conventional method.

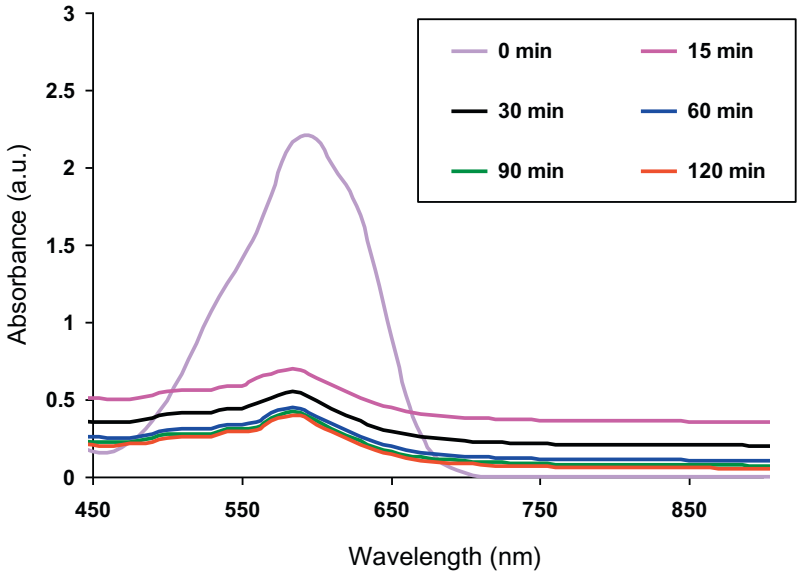

Fig. 8. Change in the absorbance spectra of crystal violet with irradiation time in presence of TiO_2 at dye concentration 30 mg/L.

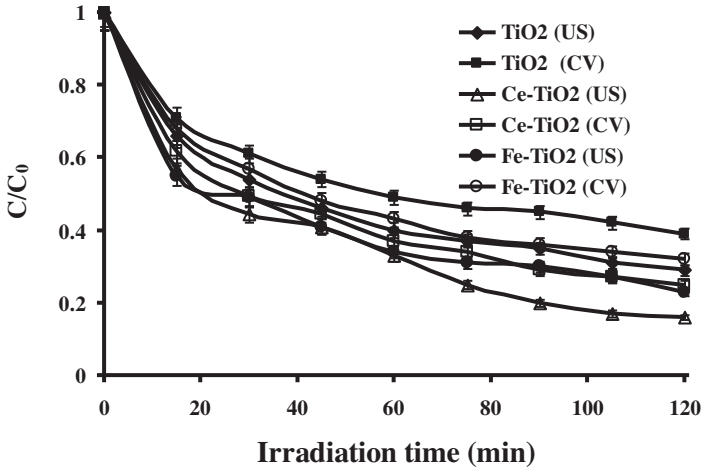

Fig. 9. Degradation vs. time decay curves of crystal violet during the photocatalytic experiments using different catalysts (dye initial concentration = 30 mg/L, pH 6.5 and catalyst dose = 0.2 g/L).

3.5.2. Effect of doping

Fig. 10 shows the variation in the relative concentration of crystal violet dye, C/C_o with UV irradiation time (C_o is the concentration after achieving the adsorption equilibrium) in the presence of cerium doping over the range of 0.4–2 mol%. It can be seen from the figure that the effectiveness of the catalyst strongly depends on the loading of Ce. The photoactivity of the catalyst increased by 10% when the content of cerium doping increased from 0.4 mol% to 0.8 mol%, however further increase resulted in a marginally decreased photoactivity of the catalyst. The observed result can be attributed to the fact that a small amount of cerium can act as a photo-generated electron trap and inhibit the hole–electron recombination [13,22]. On the other hand, the higher dopant content may become the recombination centers for the photo excited electrons, thus reducing the photocatalytic activity. Thus, an optimal dopant concentration is needed for the doping of TiO_2 and based on the present work, 0.8 mol% cerium doping was considered as the optimum doping concentration.

Fig. 11 shows the effect of iron doping concentration on the extent of degradation of crystal violet dye. As doping content of iron increased from 0.4 mol% to 1.2 mol%, the photoacivity of the catalyst increased but beyond 1.2 mol%, the activity decreased with an increase in the iron content. The observed results can be attributed to the fact that the introduction of small quantity of iron in TiO_2 is responsible for a reduction in the photo-generated hole–electron recombination rate. But at higher loadings, iron ions can serve as recombination centers and the activity steadily decreases as also demonstrated in some of the earlier investigations [2,6,24]. Thus, 1.2 mol% iron doping has been considered as the optimum doping concentration.

The high activities of the Fe and Ce doped TiO_2 powders could be attributed to the results of the synergetic effects of doping elements, small crystallite size and good crystallization during the synthesis. In both the cases, it is seen that an excess amount of dopant at the surface of TiO_2 could notably screen the TiO_2 from the UV light and inhibit the interfacial electron and hole to transfer resulting in a low photoactivity. It is observed that the photocatalytic activity of Ce doped TiO_2 is higher than that of Fe doped TiO_2. This may be because when Ce is located in an interstitial site of TiO_2, the electron density of the doped TiO_2 may increase, which

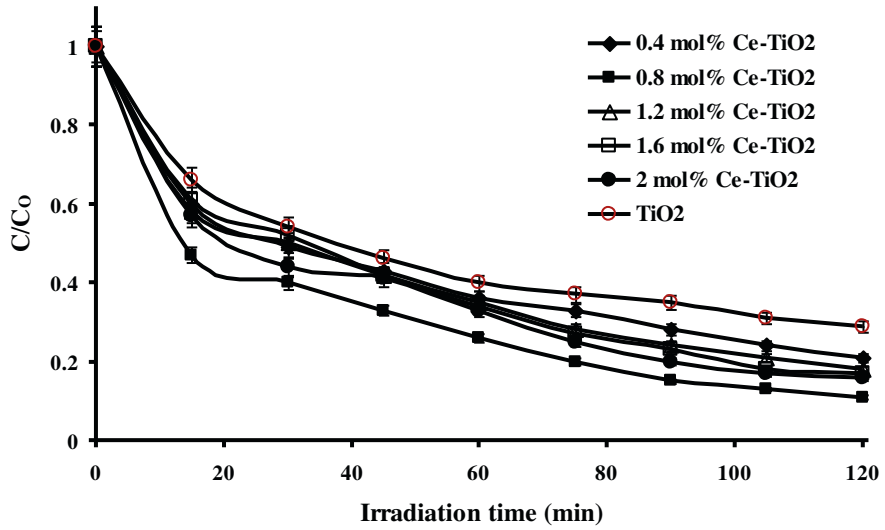

Fig. 10. Effect of cerium doping content on degradation of crystal violet dye (dye initial concentration = 30 mg/L, pH 6.5 and catalyst dose = 0.2 g/L).

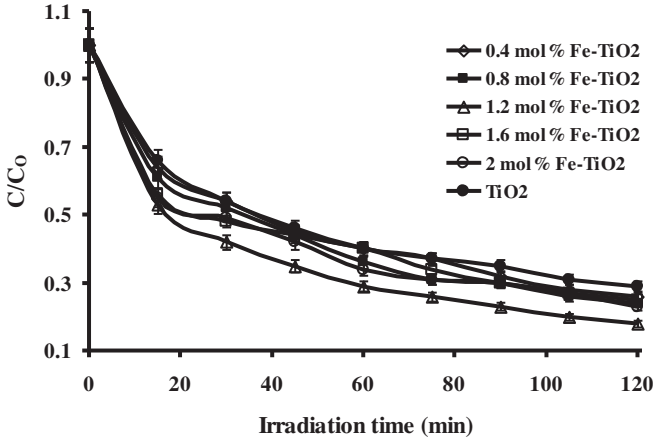

Fig. 11. Effect of iron doping content on degradation of crystal violet dye (dye initial concentration = 30 mg/L, pH 6.5 and catalyst dose = 0.2 g/L).

would increase the photocatalytic activity; while when Fe ions are located in a substitutional site of TiO_2, the electron density of the doped TiO_2 may have decreased and though TiO_2 is an n type semiconductor it may have changed into a p type semiconductor, resulting in decreased photocatalytic activity. The existence of Ce^{4+}, Fe^{3+} in the TiO_2 matrix decreases the photocurrent. According to the doping principle, the introduction of Ce^{4+}, Fe^{3+} into the matrix of TiO_2 will produce p-type micro regions [47,50], which results into change from n-type to p-type semiconductor. However, Ce 4f level in Ce–TiO_2 plays an important role in interfacial charge transfer than Fe 3f level in Fe–TiO_2 [22]. Kim et al. [51] reported that TiO_2 sample prepared by ultrasound method showed a change in surface area due to reduction in aggregation which is major change in the physical properties. Overall it can be said that the photocatalytic activity of Fe doped TiO_2 is lower than that of the Ce doped TiO_2 and the amount of doping of Fe required is also larger. Similar results are reported by Li et al. [8] for Be, Mg and Ca doped TiO_2 for photocatalytic production of hydrogen. Another reason for the difference in activities of Ce–TiO_2 and Fe–TiO_2 is that the cationic dye such as crystal violet has different charge in aqueous solution after ionization; so the electrostatic attraction or repulsion occur between the organic dye ions and the surface of catalysts, which may also result in the difference in degradation rates [23].

3.5.3. Effect of catalyst loading

To investigate the effect of catalyst loading on the degradation rate of crystal violet, experiments were conducted for three different catalyst loadings as 0.1, 0.2 and 0.3 g/L, at initial dye concentration of 30 mg/L and at pH 6.5. The obtained results have been given in Fig. 12. It can be seen from the figure that the extent of degradation increased significantly with an increase in the catalyst dosage up to a concentration of 0.2 g/L. For 0.8 mol% Ce–TiO_2 sample, 89% degradation was achieved with 0.2 g/L and maximum extent of degradation was observed to be equal to 92% at the catalyst dosage of 0.3 g/L. It was observed that there was no major difference in the degradation efficiencies for 0.2 and 0.3 g/L catalyst loadings; however 0.1 g/L catalyst loading resulted in almost 10% lesser degradation than 0.2 g/L. Similar trend was observed with Fe–TiO_2 and pure TiO_2 samples. The photodecomposition rates of pollutants are influenced by the active sites and the photoabsorption of the catalyst used in the study. Adequate loading of the catalyst can increase the generation rate of electron/hole pairs for enhancing the degradation of pollutants. At higher loadings, the catalysts may block the light irradiation, and restrain the effective usage of light for photo excitation [7,12,30]. Thus, the results indicate that an optimal dose of 0.2 g/L of the catalysts was most effective to achieve the best degradation results.

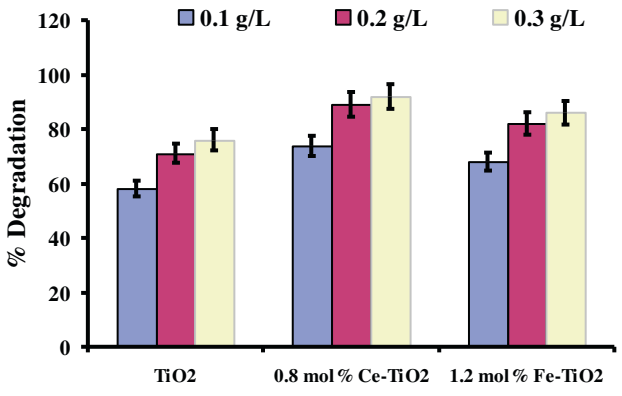

Fig. 12. Effect of catalyst loading on the crystal violet degradation (Dye initial concentration = 30 mg/L, pH 6.5).

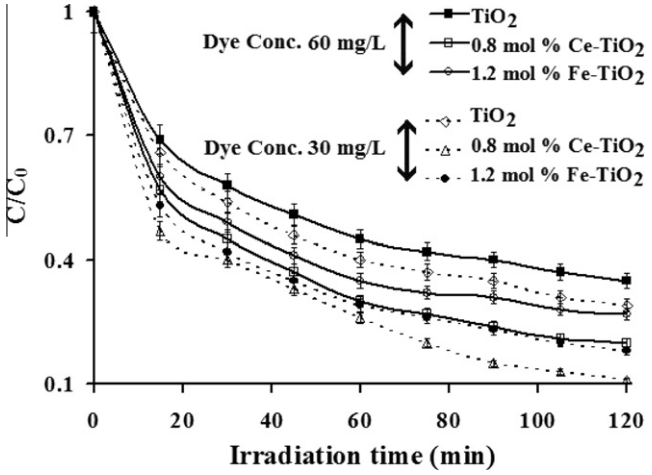

Fig. 13. Effect of initial concentration of crystal violet dye (pH 6.5 and catalyst dose = 0.2 g/L).

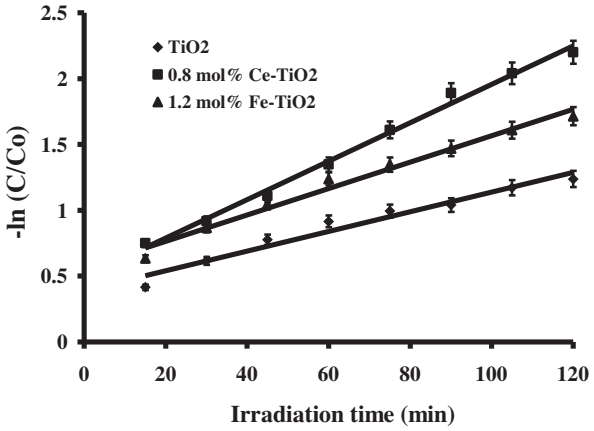

Fig. 14. Reaction kinetics for photocatalytic degradation of crystal violet (dye initial concentration = 30 mg/L, pH 6.5 and catalyst dose = 0.2 g/L).

3.5.4. Effect of initial dye concentration

Fig. 13 illustrates the variation in the relative concentration, C/C_o with irradiation time (C_o is the concentration after achieving the adsorption equilibrium) for two initial concentrations of crystal violet dye as 30 and 60 mg/L. The experiments have been conducted at pH of 6.5 and catalyst loading of 0.2 g/L. It can be seen from the figure that the higher the value of initial concentration, lower is the observed degradation rate. This negative effect may be because of the following reasons (i) when the dye concentration increases the amount of dye adsorbed on the catalyst surface increases. The increase in dye concentration will decrease the path length of photons entering the dye solution. In addition to this, at a high dye concentration, a significant amount of UV light may be absorbed by the dye molecules rather than by the catalyst particles and that reduces the efficiency of the catalytic reaction, (ii) the rate of degradation is dependent on the probability of OH**.** radicals formation on the catalyst surface and the probability of OH**.** radicals reacting with dye molecules. But at high dye concentrations the generation of OH**.** radicals on the surface of catalyst is likely to be reduced since active sites are covered by dye ions. Thus the limitation of surface sites for the reaction may control the final extent of dye degradation, (iii) the reduction in the degradation of dye can also be attributed to the filter effect caused by absorption of photon energy by the dye molecules, (iv) the relatively longer chain of crystal violet cannot completely enter the electron-hole, and thus reduces the degradation rate.

The results clearly demonstrated that the photocatalytic oxidation process is promising at low concentrations of the pollutant. This is also true for heterogeneous catalytic systems where the reaction occurs at the interface between two phases. [2,7,12]

3.5.5. Kinetics of the degradation

Kinetics of photocatalytic degradation of crystal violet has also been investigated. The pseudo-first order reaction kinetics can be represented by the following equation

$$-\ln\left(\frac{C}{C_0}\right) = kt \quad (1)$$

where C is the final concentration (mg/L) of crystal violet after irradiation, C_0 is the initial concentration (mg/L) of crystal violet (after reaching the adsorption equilibrium but prior to irradiation), t is the irradiation time (min) and k is the apparent reaction rate constant (min^{-1}). The kinetic studies have been performed for the sonochemically prepared catalysts with the optimum doping content for cerium and iron as 0.8 and 1.2 mol% respectively and also comparison has been done with the sonochemically synthesized pure TiO_2. Fig. 14 gives the first-order reaction kinetics for photocatalytic degradation of crystal violet dye for the three catalyst samples. The obtained rate constants have been reported in Table 1. It can be seen that the rate constant for 0.8 mol% Ce–TiO_2 sample was twice as compared to that of pure TiO_2 and for 1.2 mol% Fe–TiO_2 it was 0.010 min^{-1}, which is about 45% more as compared to the pure TiO_2. The results have clearly established the better efficacy of the doped photocatalyst as compared to the pure form of TiO_2.

Table 1
Rate constants for first order kinetics.

Catalyst	Rate constant (min^{-1})	R^2 values
Pure TiO_2	0.007	0.962
1.2 mol% Fe–TiO_2	0.010	0.983
0.8 mol% Ce–TiO_2	0.014	0.990

4. Conclusions

Nano-sized Fe, Ce-doped and undoped TiO_2 particles were synthesized by sonochemical and conventional methods using titanium isopropoxide as a starting material. Catalysts prepared by sonochemical method exhibited higher photocatalytic activity as compared to the catalysts prepared by conventional method. The presence of Fe and Ce in the TiO_2 structure caused a significant absorption shift towards the visible region. An optimum quantity of dopant obtained was 0.8 mol% Ce–TiO_2 and 1.2 mol% Fe–TiO_2 where maximum photoactivity could be observed. Also, an optimal dosage of 0.2 g/L of the photocatalyst was observed whereas lower initial concentration of the dye was favorable for giving higher extents of degradation. The photocatalytic degradation followed first-order kinetics and overall it can be said that crystal violet dye was effectively degraded (more than 85% degradation) within 120 min of UV irradiation.

Acknowledgements

SRS acknowledges the support of Indian Academy of Sciences, Bangalore to carry out this work under Summer Research Fellowship scheme for Teachers (2011). SHS acknowledges the financial support of the Ministry of Environment and Forest (MoEF, Govt of India).

References

[1] R. Chand, E. Obuchi, K. Katoh, H.N. Luitel, K. Nakano, Enhanced photocatalytic activity of TiO_2/SiO_2 by the influence of Cu-doping under reducing calcination atmosphere, Catal. Commun. 13 (2011) 49–53.

[2] M. Asiltürk, F. Sayılkan, E. Arpac, Effect of Fe^{3+} ion doping to TiO_2 on the photocatalytic degradation of Malachite Green dye under UV and vis-irradiation, J. Photochem. Photobiol. A: Chem. 203 (2009) 64–71.

[3] M. Asilturk, F. Sayılkan, S. Erdemoglu, M. Akarsu, H. Sayılkan, M. Erdemoglu, E. Arpac, Characterization of the hydrothermally synthesized nano- TiO_2 crystallite and the photocatalytic degradation of Rhodamine B, J. Hazard. Mater. B129 (2006) 164–170.

[4] S. Rengaraj, X.Z. Li, Enhanced photocatalytic activity of TiO_2 by doping with Ag for degradation of 2, 4, 6-trichlorophenol in aqueous suspension, J. Mol. Catal. A: Chem. 243 (2006) 60–67.

[5] F. Wang, K. Zhang, Reduced graphene oxide- TiO_2 nanocomposite with high photocatalystic activity for degradation of rhodamine B, J. Mol. Catal. A: Chem. 345 (2010) 101–107.

[6] M. Zhou, J. Yu, B. Cheng, Effects of Fe-doping on the photocatalytic activity of mesoporous TiO_2 powders prepared by an ultrasonic method, J. Hazard. Mater. B137 (2006) 1838–1847.

[7] H. Wang, J. Niu, X. Long, Y. He, Sonophotocatalytic degradation of methyl orange by nano-sized Ag/ TiO_2 particles in aqueous solutions, Ultrason. Sonochem. 15 (2008) 386–392.

[8] Y. Li, S. Peng, F. Jiang, G. Lu, S. Li, Effect of doping TiO_2 with alkaline-earth metal ions on its photocatalytic activity, J. Serb. Chem. Soc. 72 (2007) 393–402.

[9] U.G. Akpan, B.H. Hameed, Enhancement of the photocatalytic activity of TiO_2 by doping it with calcium ions, J. Colloid Interface Sci. 357 (2011) 168–178.

[10] H.K. Shon, S. Vigneswaran, J. Kandasamy, M.H. Zareie, J.B. Kim, D.L. Cho, J.H. Kim, Preparation and characterization of titanium dioxide (TiO_2) from sludge produced by $TiCl_4$ flocculation with $FeCl_3$, $Al_2(SO_4)_3$ and $Ca(OH)_2$ coagulant aids in wastewater, Sep. Sci. Technol. 44 (2009) 1525–1543.

[11] Y.H. Peng, G.F. Huang, W.Q. Huang, Visible-light absorption and photocatalytic activity of Cr-doped TiO_2 nanocrystal films, Adv. Powder Technol. 23 (2010) 8–12.

[12] M.A. Barakat, H. Schaeffer, G. Hayes, S. Ismat-Shaha, Photocatalytic degradation of 2-chlorophenol by Co-doped TiO_2 nanoparticles, App. Catal. B: Environ. 57 (2004) 23–30.

[13] A.M.T. Silva, C.G. Silva, G. Drazić, J.L. Faria, Ce-doped TiO_2 for photocatalytic degradation of chlorophenol, Catal. Today 144 (2009) 13–18.

[14] M.A. Rauf, M.A. Meetani, S. Hisaindee, An overview on the photocatalytic degradation of azo dyes in the presence of TiO_2 doped with selective transition metals, Desalination 276 (2011) 13–27.

[15] S. Anandan, M. Ashokkumar, Sonochemical synthesis of Au–TiO_2 nanoparticles for the sonophotocatalytic degradation of organic pollutants in aqueous environment, Ultrason. Sonochem. 16 (2009) 316–320.

[16] K. Kocí, K. Mateju, L. Obalová, S. Krejcíková, Z. Lacný, D. Plachá, L. Capek, A. Hospodková, O. Solcov, Effect of silver doping on the TiO_2 for photocatalytic reduction of CO_2, App. Catal. B: Environ. 96 (2010).

[17] Y. Li, C. Xie, S. Peng, G. Lu, S. Li, Eosin Y-sensitized nitrogen-doped TiO_2 for efficient visible light photocatalytic hydrogen evolution, J. Mol. Catal. A: Chem. 282 (2008) 117–123.

[18] H.K. Shon, D.L. Cho, S.H. Na, J.B. Kim, H.J. Park, J.H. Kim, Development of a novel method to prepare Fe- and Al-doped TiO_2 from wastewater, J. Ind. Eng. Chem. 15 (2009) 476–482.

[19] S. Chang, W. Liu, Surface doping is more beneficial than bulk doping to the photocatalytic activity of vanadium-doped TiO_2, App. Catal. B: Environ. 101 (2011) 333–342.

[20] N. Venkatachalam, M. Palanichamy, B. Arabindoo, V. Murugesan, Enhanced photocatalytic degradation of 4-chlorophenol by Zr^{4+} doped nano TiO_2, J. Mol. Catal. A: Chem. 266 (2007) 158–165.

[21] A. Zaleska, Doped- TiO_2: a review, Recent Patents on Engineering 2 (2008) 157–164.

[22] Z.L. Shi, C. Du, S.H. Yao, Preparation and photocatalytic activity of cerium doped anatase titanium dioxide coated magnetite composite, J. Taiwan Inst. Chem. Eng. 42 (2011) 652–657.

[23] J. Wang, Y. Lv, L. Zhang, B. Liu, R. Jiang, G. Han, R. Xu, X. Zhang, Sonocatalytic degradation of organic dyes and comparison of catalytic activities of CeO_2/TiO_2, SnO_2/TiO_2 and ZrO_2/ TiO_2 composites under ultrasonic irradiation, Ultrason. Sonochem. 17 (2010) 642–648.

[24] M.S. Nahar, K. Hasegawa, S. Kagaya, S. Kuroda, Comparative assessment of the efficiency of Fe-doped TiO_2 prepared by two doping methods and photocatalytic degradation of phenol in domestic water suspensions, Sci. Technol. Adv. Mater. 8 (2007) 286–291.

[25] T.K. Ghorai, S.K. Biswas, P. Pramanik, Photooxidation of different organic dyes (RB, MO, TB, and BG) using Fe (III)-doped TiO_2 nanophotocatalyst prepared by novel chemical method, Appl. Surf. Sci. 254 (2008) 7498–7504.

[26] N.D. Abazovic, L. Mirenghi, I.A. Jankovic, N. Bibic, D.V. Sojic, B.F. Abramovic, M.I. Comor, Synthesis and characterization of rutile TiO_2 nanopowders doped with iron ions, Nanoscale Res. Lett. 4 (2009) 518–525.

[27] C.L. Luu, Q.T. Nguyen, S.T. Ho, Synthesis and characterization of Fe-doped TiO_2 photocatalyst by the sol–gel method, Adv. Nat. Sci. Nanosci.: Nanotechnol. 1 (2010) 01–05.

[28] Q.H. Zhang, W.D. Han, Y.J. Hong, J.G. Yu, Photocatalytic reduction of CO_2 with H_2O on Pt-loaded TiO_2 catalyst, Catal. Today 148 (2009) 335–340.

[29] X. Li, R. Xiong, G. Wei, Preparation and photocatalytic activity of nanoglued Sn-doped TiO_2, J. Hazard. Mater. 164 (2009) 587–591.

[30] F.I. Kiriakidou, D.I. Kondarides, X.E. Verykios, The effect of operational parameters and TiO_2-doping on the photocatalytic degradation of azo-dyes, Catal. Today 54 (1999) 119–130.

[31] S. Liu, X. Chen, A visible light response TiO_2 photocatalyst realized by cationic S-doping and its application for phenol degradation, J. Hazard. Mater. 152 (2008) 48–55.

[32] B.N. Narayanan, Z. Yaakob, R. Koodathil, S. Chandralayam, S. Sugunan, F.K. Saidu, V. Malayattil, Photodegradation of methylorange over zirconia doped TiO_2 using solar energy, Eur. J. Sci. Res. 28 (2009) 566–571.

[33] X.K. Wang, C. Wang, W.L. Guo, Sonochemical synthesis of nitrogen doped TiO_2 at a low temperature, Adv. Mater. Res. 356 (2012) 403–406.

[34] J. Yu, M. Zhou, B. Cheng, H. Yu, X. Zhao, Ultrasonic preparation of mesoporous titanium dioxide nanocrystalline photocatalysts and evaluation of photocatalytic activity, J. Mol. Catal. A: Chem. 227 (2005) 75–80.

[35] X. Chen, S.S. Mao, Titanium dioxide nanomaterials: synthesis, properties, modifications, and applications, Chem. Rev. 107 (2007) 2891–2959.

[36] W. Huang, X. Tang, Y. Wang, Y. Koltypin, A. Gedanken, Selective synthesis of anatase and rutile via ultrasound irradiation, Chem. Commun. 15 (2000) 1415–1416.

[37] J.C. Yu, J. Yu, W. Ho, L. Zhang, Preparation of highly photocatalytic active nano-sized TiO_2 particles via ultrasonic irradiation, Chem. Commun. 19 (2001) 1942–1943.

[38] H. Li, G. Liu, S. Chen, Q. Liu, Novel Fe doped mesoporousTiO_2 microspheres: Ultrasonic–hydrothermal synthesis, characterization, and photocatalytic properties, Physica E 42 (2010) 1844–1849.

[39] B. Neppolian, Q. Wang, H. Jung, H. Choi, Ultrasonic-assisted sol-gel method of preparation of TiO_2 nano-particles: characterization, properties and 4-chlorophenol removal application, Ultrason. Sonochem. 15 (2008) 649–658.

[40] Y. Zhu, H. Li, Y. Koltypin, Y.R. Hacohen, A. Gedanken, Sonochemical synthesis of titania whiskers and nanotubes, Chem. Commun. 24 (2001) 2616–2617.

[41] W. Huang, X. Tang, I. Felner, Y. Koltypin, A. Gedanken, Preparation and characterization of FexOy-TiO_2 via sonochemical synthesis, Mater. Res. Bull. 37 (2002) 1721–1735.

[42] Y. Xie, C. Yuan, Visible-light responsive cerium ion modified titania sol and nanocrystallites for X-3B dye photodegradation, Appl. Catal. B: Environ. 46 (2003) 251–259.

[43] S. Liu, X. Chen, Preparation of N-doped visible-light response nanosize TiO_2 photocatalyst using the acid-catalyzed hydrolysis method, Chin. J. Catal. 27 (2006) 697–702.

[44] Z. Shi, H. Lai, S. Yao, S. Wang, Photocatalytic Activity of Fe and Ce Co-doped Mesoporous TiO_2 Catalyst under UV and Visible Light, J. Chin. Chem. Soc. 59 (2012) 1–8.

[45] J.C.S. Wu, C.H. Chen, A visible-light response vanadium-doped titania nanocatalyst by sol–gel method, J. Photochem. Photobiol. A Chem 163 (2004) 509–515.

[46] M. Popa, E. Indrea, P. Pascuta, V. Cosoveanu, I.C. Popescu, V. Danciu, Fe, Ce, and Cu influence on morpho-structural and photoctalytic properties of TiO_2 aerogels, Rev. Roum. Chim. 55 (2010) 369–375.

[47] D.V. Pinjari, A.B. Pandit, Room temperature synthesis of crystalline CeO_2 nanopowder: advantage of sonochemical method over conventional method, Ultrason. Sonochem. 18 (2011) 1118–1123.

[48] J. Bandara, V. Nadtochenko, J. Kiwi, C. Pulgarin, Dynamics of oxidant addition as an important parameter in the modelization of dye mineralization (orange II) via advanced oxidation technologies, Water Sci. Technol. 35 (1997) 87–93.

[49] E.G. Janzen, Y. Kotake, R.D. Hinton, Stabilities of the hydroxyl radicals spin adducts of PBN-type spin traps, Free Radical Biol. Med. 12 (1992) 169–173.

[50] P. Yang, C. Lu, N. Hua, Y. Du, Titanium dioxide nanoparticles co-doped with Fe^{3+} and Eu^{3+} ions for photocatalysis, Mater. Lett. 57 (2002) 794–801.

[51] S.Y. Kim, T.S. Chang, C.H. Shin, Enhancing effects of ultrasound treatment on the preparation of TiO_2 Photocatalysts, Catal. Lett. 118 (2007) 224–230.